

Infrared Spectra and Structures of Large Water Clusters

J. P. Devlin* and C. Joyce

Department of Chemistry, Oklahoma State University, Stillwater, Oklahoma 74078

V. Buch*

The Fritz Haber Institute for Molecular Dynamics, The Hebrew University, Jerusalem 91904, Israel

Received: December 16, 1999

Infrared spectra have been determined for aerosol ice samples with particles that vary in average diameter down to ~ 2 nm. The aerosol spectra, obtained at 100 K, show that the crystalline core of the average particle decreases rapidly with decreasing particle size and vanishes near 4 nm (or 1000 molecules). Consequently, the combined FT-IR spectrum of the surface and subsurface regions has been observed directly for the first time and observed to be nearly invariant to ~ 3 nm. Using a polarizable water potential, the structure and spectra of a 1000 molecule cluster has been simulated. The starting point was an approximately spherical cubic ice structure, which was subjected to relaxation by molecular dynamics. The resulting lower energy structure includes a disordered surface layer and an interior that clearly retains a degree of oxygen order. The simulated spectrum of the cluster is separable into components resembling the surface, subsurface, and core ice experimental spectra. The combined results support the description of ice nanoparticles as a central crystalline core surrounded by a subsurface region and a strongly disordered outer surface layer. The virtually crystalline subsurface, though strained by interaction with the surface, persists to a size of a few hundred H₂O.

Introduction

Characterizing water clusters, (H₂O)_n with *n* in the range 2 to several tens, has been and continues to be a very active field of study.¹ Also, in recent years there have been a number of diffraction^{2,3} and infrared^{4,5} investigations of water particles in the 6–100 nm range. On the basis of our infrared studies, the nearly spherical particles⁶ have been characterized as having a cubic ice core and a disordered surface joined together by a transition, or subsurface, region.^{4,5} For a 20 nm particle, a favorite target of our previous FT-IR/simulation studies, $\sim 75\%$ of the water molecules are part of the crystalline core while the surface accounts for $\sim 10\%$ and the remainder are in the subsurface category. With an increased understanding of the small- and medium-sized clusters, together with an accumulation of data for nanocrystals, there is a growing interest in closing the knowledge gap for the range from ~ 20 to 1000 molecules⁷ (the latter corresponds to ~ 4 nm very large clusters).

Particularly informative data for clusters in this size range include the electron diffraction patterns determined by Torchet et al.³ These data, for clusters within an expansion beam, suggest that clusters larger than ~ 290 water molecules are required for any crystalline component to be present. A crystalline component was reported starting with ~ 900 water molecules.

There has been little published vibrational spectroscopic data for very large water clusters since the pioneering predissociation measurements of Watts et al.,⁸ though Buck et al. have examined the intermolecular modes,⁹ core-level electronic spectra have been reported very recently¹⁰ and optical constants have been evaluated for 0.3 μm ice particles.¹¹ The spectra of Watts, as well as that of Page et al.¹² and Huisken et al.¹³ for medium-sized H₂O clusters, showed that absorption extends from near 3050 to 3720 cm⁻¹, but no effort (beyond invoking obvious

analogies with small clusters and condensed phases) was made to assign the several subbands.

The purpose of this communication is to report 4 cm⁻¹ FT-IR spectra for clusters ranging from 2 to 40 nm, and to give an interpretation of the various components of these spectra. The interpretation will be based on simulations of a 1000 molecule cluster, plus trends observed in spectra with decreasing particle size, and published results for larger nanocrystals. The new experimental data are for D₂O clusters as well as 18% HDO in H₂O clusters. The latter can be compared directly with the most informative simulated spectra, as the interpretation of the HDO spectrum is facilitated by the absence of intramolecular and significantly reduced intermolecular coupling of the O–D oscillators in the largely H₂O environment. *The frequency of an isotopically isolated OD stretch reflects directly the local strength of the hydrogen bond.*

The 2–8 nm ice particles have been prepared as aerosols by rapid expansion of a 0.1% mixture of water vapor in He(g) or N₂(g) into a thick-walled cluster cell held at 100 K within a vacuum container. The cluster size has been chosen by varying the loading pressure from 60 to 400 Torr. As in previous studies, the average size of the clusters has been determined from integrated infrared band intensities for monolayer adsorbed CF₄.^{5a} As in a supersonic free jet,^{2,3} the particles form as liquid droplets (with a log-normal size distribution) that freeze while cooling rapidly toward temperatures near 100 K.

Results and Discussion

Experimental Spectra. The influence of decreasing particle size on the infrared spectrum of a very large ice cluster is apparent from Figure 1. The top spectrum for a 16 nm particle appears to be that of crystalline D₂O ice¹⁴ with the three

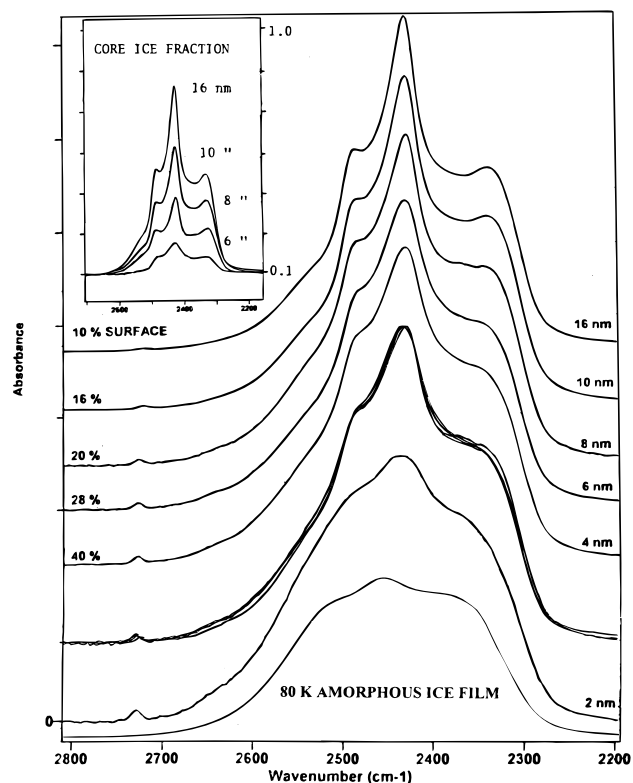


Figure 1. FT-IR spectra in the O–D stretch-mode region of D_2O particles in the 16 to 2 nm range as aerosols at 100 K and of an amorphous ice thin film (bottom). The overlaid spectra are for the 4, 6, 8, and 10 nm particles with the crystalline core component removed (see text). The inset shows spectra of the core components of the larger particles obtained by subtraction of the 4 nm particle spectrum.

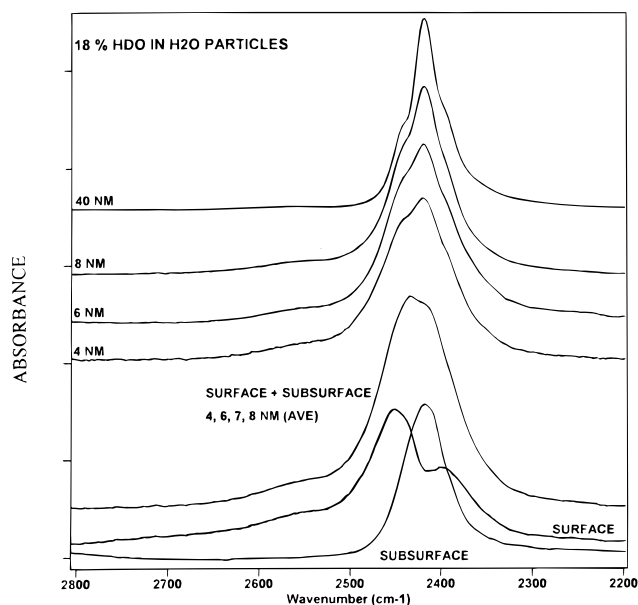


Figure 2. As in Figure 1, but for 18% HDO in H_2O particles of the indicated diameter. Also shown is the average of the small-particle spectra (after removal of the crystalline core component using the 40 nm spectrum) and the surface and subsurface components of this spectrum.

prominent features at 2490, 2430, and 2330 cm^{-1} . In fact, less than 75% of the total intensity of the O–D stretch band for such particles results from interior crystalline ice, with the surface and subsurface both contributing significantly to the spectrum.^{4,5} The nature of these underlying spectral components becomes clear as the particle size is reduced from 16 nm toward

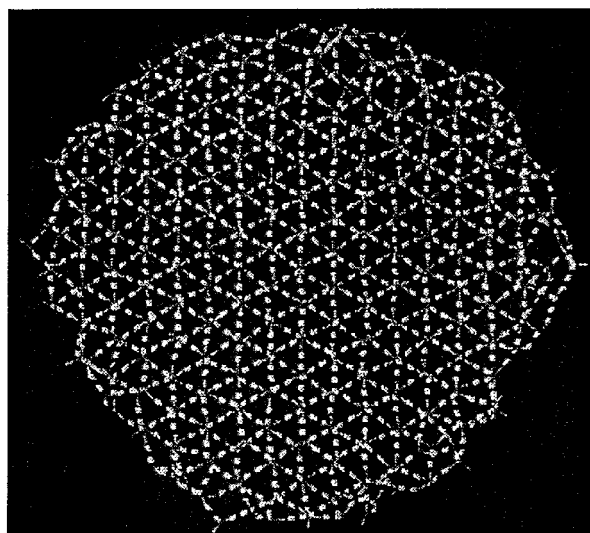
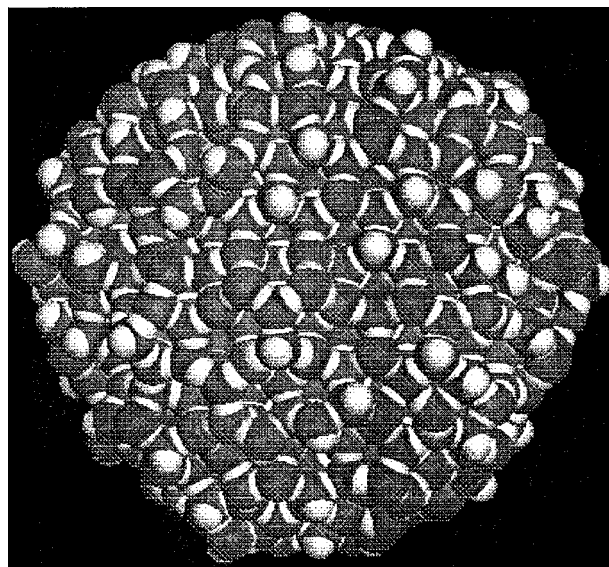


Figure 3. Relaxed cluster structure. Top: space filling model, demonstrates surface disorder. Bottom: stick model of a 1.1 nm thick middle slice of the cluster, demonstrating the largely ordered interior and subsurface.

4 nm. As one would anticipate from the early electron diffraction results,³ the crystalline core component of the spectrum decreases rapidly, becoming a minor component at 6 nm and nearly vanishing at 4 nm. It follows that the 4 nm spectrum is dominantly ($\sim 90\%$) that of the combined surface and subsurface.

As the ice particle size is reduced, a leading question is whether the nature of the remaining surface and subsurface components is unchanged; or does the subsurface evolve toward an amorphous ice structure while the surface becomes even more highly disordered? From comparison with the (bottom) amorphous ice spectrum, it is clear that the spectrum of the 2 nm particles (next to the bottom of Figure 1) reflects the presence of an amorphous ice component.¹⁴ By contrast, the close match of the overlaid spectra near the bottom of Figure 1, obtained by removing the interior ice component from the spectra of the 4, 6, 8, and 10 nm particles, suggest that (1) the surface and subsurface spectra do not vary greatly with particle size through this range and (2) the relative amounts of the surface and subsurface components are fairly constant. The inset of Figure 1 shows the approximate fractional component that is interior ice, for particles ranging in size from 6 to 16 nm, as determined

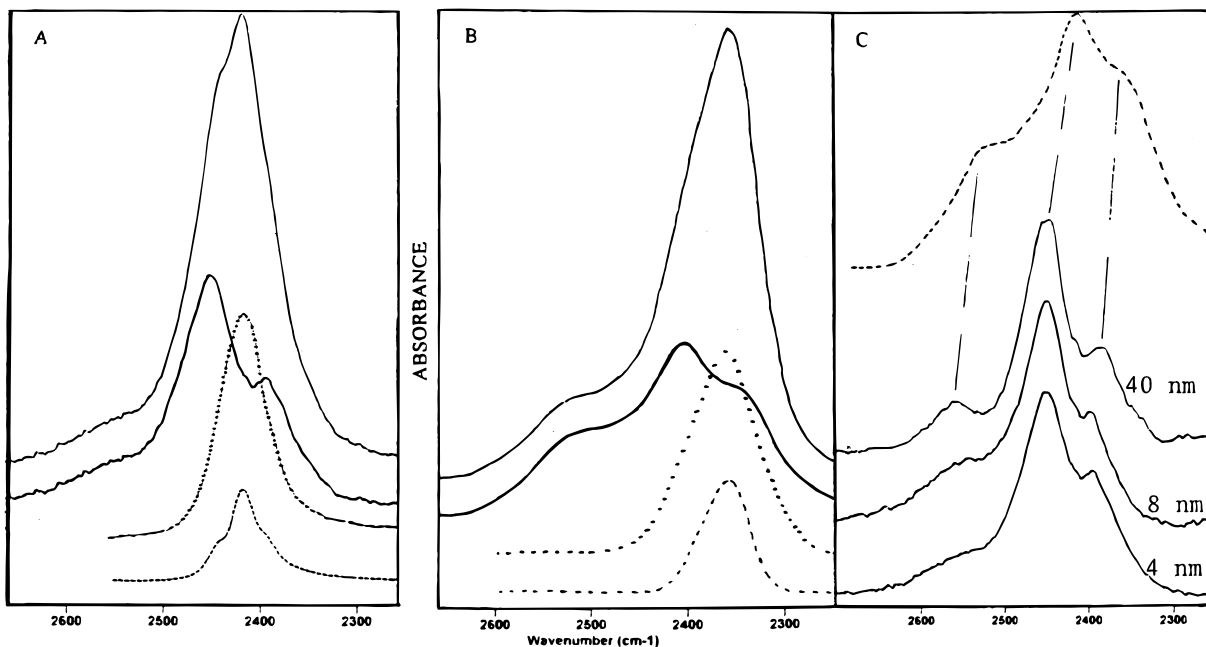


Figure 4. Comparison of the experimental (A; top) and simulated (B; top) spectra of the “decoupled” O–D stretch mode of HDO for a ~ 1000 molecule cluster. The experimental spectra are for 18% HDO in primarily H₂O ice particles at 100 K. The bottom three spectra of A and B show, to scale, the surface (—), subsurface (···), and interior (---) components. In (C), the computed cluster surface spectrum (top) is compared with surface spectra of particles of the indicated diameters.

by direct subtraction of the spectrum of the 4 nm particles from the other spectra.

These D₂O data indicate that the surface and subsurface spectra do not change significantly in form as long as there is a crystalline core. In fact, the form of the surface and subsurface spectra are unchanged for particles as small as ~ 3 nm, for which no core component is observable. This simplifies the separation of the spectra for the various sized particles into the three components of surface, subsurface, and interior. The approach used is demonstrated for the O–D stretch of “decoupled” HDO in Figure 2. The top four spectra of Figure 2, like those of D₂O in Figure 1, show the effect of particle size on the raw spectra of the ice aerosols. Removal of the crystalline core spectrum (of the 40 nm particles) from the average of the three small-particle spectra gives the combined surface and subsurface spectrum shown in Figure 2. The subtraction of the subsurface spectrum, known from studies of larger ice nanocrystals,^{5b} then reveals the surface spectrum. The separated spectra can then be used to resolve a spectrum of an arbitrary ice aerosol into the three components with minor residual error.

Computations of Structure and Spectra; Comparison to Experiment. It is assumed in this study that the particle adopts a nearly spherical geometry, to reduce its surface area/energy. The first question addressed is the surface structure, given a crystalline interior. The starting point was a spherical particle cut out of the cubic ice structure, of 4 nm diameter and including 979 molecules. Ice Ic is known to be proton disordered; only O atoms form a periodic pattern, while the orientations are random within the requirement of four hydrogen bonds per molecule.¹⁵ The algorithm used to generate a proton-disordered ice Ic model is given in ref 16. Minimizations and molecular dynamics simulations described below were carried out using a polarizable potential and methods described in refs 16 and 17.

The initial spherical surface includes numerous dangling H and O atoms and is energetically unfavorable. Relaxation can be obtained by minimization of the potential energy; as a result, the cluster energy decreases by 570 kcal/mol of clusters and

the number of molecules of coordination lower than 4 decreases from 321 to 234. However further energy lowering was obtained by allowing for more extensive surface restructuring. The restructuring was effected by heating the cluster by molecular dynamics to some temperature T_1 (at which the surface molecules just become mobile); a classical trajectory was then run for time t , followed by slow recooling and minimization. The lowest energy final structures were found for an initial structure of a relatively low dipole (17.5 D), T_1 near 190 K, and t of a few tens of picoseconds. As a result, the energy was lowered another 190 kcal/mol with respect to the initial minimum, and the number of low coordinated molecules was further reduced (by ~ 40).

The resulting relaxed structure is shown in Figure 3. The space-filling model demonstrates surface disorder, while the stick model with H-bonds shows substantial ordering of the interior. While the structure is unlikely to represent the absolute energy minimum, the calculation shows that significant lowering is obtained by further removal of surface molecules away from crystalline positions.

The spectrum of the relaxed structure was calculated using a scheme¹⁸ developed to study $n = 8-10$ cage clusters. The bond frequency ω is calibrated as a function of the electric field component E_{\parallel} along the OD bond, at the D atom; the field is calculated at a cluster minimum, using the permanent charges and the induced dipoles of the polarizable potential. (This parametrization was suggested by past ab initio studies.¹⁹) The scheme is designed for relatively rigid clusters, which are localized near a single minimum. A function $\omega(E_{\parallel})$ was found, such that both the spectra of $n = 7-10$ clusters^{18,20} and of the 1000 molecule clusters are reproduced at a semiquantitative level. The coupling between OD bonds was neglected. The calculated spectra are shown in Figure 4B.

While the computational scheme clearly requires further improvement (the calculated spectra are too broad), it was possible to reproduce qualitative features of the experiment such as the increasing broadening of the spectra for the sequence interior–subsurface–surface (see Figure 4). Moreover, in

qualitative accord with experiment, the H-bonded **surface** spectrum includes both a low and a high-frequency feature in addition to a central peak, which is shifted to the blue with respect to the interior band. The highest frequency feature is due to outermost molecules that stick out of the surface; these include 3-coordinated molecules with a dangling O (d-O) and 4-coordinated H₂O with a strongly distorted coordination shell (S4). The two lower frequency features are due to 4-coordinated inner surface molecules, while the low frequency tail is contributed mostly by the bonded OD of 3-coordinated molecules with a dangling D. Interestingly, the d-O/S4 feature near 2560 cm⁻¹ weakens with the decreasing cluster size (Figure 4C); a similar result seems valid for the weak dangling-D feature at 2713 cm⁻¹ (not shown). The calculated d-O feature appears to be too intense, which suggests that in reality relaxation toward elimination of low-coordinated molecules is more extensive than in the calculated model.

The division to “surface”, “subsurface”, and “interior” (Figure 4B) was made at radii of 1.4 and 0.9 nm. At these values best agreement was attained with the experimental band shapes. The calculated percentages of molecules contributing to the three components are 64%, 26%, and 10%; the corresponding values obtained from integrated band areas of ~4 nm particles are 60%, 28%, and 11%, respectively. The **surface** disorder is reflected by a distribution of O···O···O angles between the adjacent hydrogen bonds, which has a standard deviation of 14° (as compared to 6° only for the combined subsurface and interior). The subsurface is structurally similar to the crystalline interior, except for a somewhat broader distribution of O···O···O angles and O···O nearest neighbor distances.

Finally, one may try to relate the present results to a recent computational study of Tanaka et al.²¹ of water clusters up to 864 molecules (employing TIP4P). It was argued there that, up to ~1000 molecules, spherical particles are less favorable energetically than disklike sandwich structures composed of two connected hexagonal layers, without any dangling atoms (except at edges). However, in that study, the **spherical** cluster energy was calculated at the local energy minimum, and a possibility of further surface relaxation was not considered. According to our calculations, energy lowering due to such relaxation is of the order of the energy difference calculated²¹ between the two cluster forms. Moreover, both our spectroscopic studies and the electron diffraction data of Torchet³ indicate, for the “few hundred” regime, three-dimensional amorphous structures, rather than ordered sandwich structures with very few dangling atoms (e.g., the 2726 cm⁻¹ band of Figure 1 signals a large population of such atoms for all particle sizes, though the surface concentration decreases by ~40% between 20 and 4 nm).

Conclusions

The main conclusion from the infrared spectra and simulations for ~1000 molecule water clusters is that they are composed of disordered surface, strained subsurface, and crystalline core

regions. The subsurface is a nucleated structure similar to the crystalline core, except for slightly distorted hydrogen bonds from interaction with the surface. Even in the absence of the core region, this “crystalline” subsurface region exists down to a cluster size of ~3 nm or ~500 molecules. The core and subsurface structures match those of ice nanocrystals,^{4,5} while the disordered surface is similar, though with a reduced population of dangling O and H atoms. These conclusions are compatible with the electron diffraction data for very large clusters.^{2,3}

Acknowledgment. Support of the National Science Foundation, Grant 9617120, and the Binational Science Foundation, Grant 9800208, is gratefully acknowledged.

References and Notes

- (1) See, for example, references cited in: (a) Sadlej, J.; Buch, V.; Kazimirski, J. K.; Buck, U. *J. Phys. Chem. A* **1999**, *103*, 4933, (b) Liu, K.; Brown, M. G.; Saykally, R. J. *J. Phys. Chem. A* **1997**, *101*, 8995, (c) Gruenloh, C. J.; Carney, J. R.; Hagemester, R. C.; Arrington, C. A.; Zwier, T. S.; Fredericks, S. Y.; Wood, J. T.; Jordan, K. D. *J. Chem. Phys.* **1998**, *109*, 6601, (d) Gregory, J. K.; Clary, D. C. *J. Phys. Chem.* **1996**, *100*, 18014, and (e) Scheiner, S. *Annu. Rev. Phys. Chem.* **1994**, *45*, 23.
- (2) Huang, J.; Bartell, L. S. *J. Phys. Chem.* **1995**, *99*, 3924.
- (3) Torchet, G.; Schwartz, P.; Farges, J.; de Feraudy, M. F.; Raoult, B. *J. Chem. Phys.* **1983**, *79*, 6196.
- (4) Devlin, J. P.; Buch, V. *J. Phys. Chem. B* **1997**, *101*, 6095.
- (5) (a) Buch, V.; Delzeit, L.; Blackledge, C.; Devlin, J. P. *J. Phys. Chem.* **1996**, *100*, 3732. (b) Delzeit, L.; Devlin, J. P.; Buch, V. *J. Chem. Phys.* **1997**, *107*, 3726.
- (6) Private communication of transmission electron micrograph data for ice nanocrystals; David Blake and Lance Delzeit, NASA Ames, Moffett Field, California.
- (7) See, e.g.: Eggen, B. R.; Marks, A. J.; Murrel, J. N.; Farantos, S. C. *Chem. Phys. Lett.* **1994**, *219*, 247. Sremaniak, L. S.; Perera, L.; Berkowitz, M. L. *J. Chem. Phys.* **1996**, *105*, 3715. Wales, D. J.; Hodges, M. P. *Chem. Phys. Lett.* **1998**, *286*, 65. Baba, A.; Tanaka, J.; Saito, S.; Matsumoto, M.; Ohmine, I. *J. Mol. Liq.* **1998**, *77*, 95.
- (8) Coker, D. F.; Miller, R. E.; Watts, R. O. *J. Chem. Phys.* **1985**, *82*, 3554.
- (9) Brudermann, J.; Lohbrandt, P.; Buck, U.; Buch, V. *Phys. Rev. Lett.* **1998**, *980*, 2821.
- (10) Bjornholm, O.; Federmann, F.; Kakar, S.; Moller, T. *J. Chem. Phys.* **1999**, *111*, 546.
- (11) Clapp, M. L.; Miller, R. E.; Worsnop, D. R. *J. Phys. Chem.* **1995**, *99*, 6317.
- (12) Page, R. H.; Vernon, M. F.; Shen, Y. R.; Lee, Y. T. *Chem. Phys. Lett.* **1987**, *141*, 1.
- (13) Huisken, F.; Mohammad-Pooran, S.; Werhahn, O. *Chem. Phys.* **1998**, *239*, 11.
- (14) Bergren, M. S.; Schuh, D.; Sceats, M. G.; Rice, S. A. *J. Chem. Phys.* **1978**, *69*, 3477.
- (15) Hobbs, P. V. *Ice Physics*; Clarendon: Oxford, U.K., 1974.
- (16) Buch, V.; Sandler, P.; Sadlej, J. *J. Phys. Chem. B* **1998**, 8641.
- (17) Witek, H.; Buch, V. *J. Chem. Phys.* **1999**, *110*, 3168.
- (18) Buck, U.; Ettischer, I.; Melzer, M.; Buch, V.; Sadlej, J. *Phys. Rev. Lett.* **1998**, *80*, 2578.
- (19) Hermansson, K.; Lingren, J.; Probst, M. M. *Chem. Phys. Lett.* **1995**, *233*, 371.
- (20) Brudermann, J.; Melzer, M.; Buck, U.; Kazimirski, J.; Sadlej, J.; Buch, V. *J. Chem. Phys.* **1999**, *110*, 10649.
- (21) Tanaka, H.; Yamamoto, R.; Koga, K.; Zeng, X. C. *Chem. Phys. Lett.* **1999**, *304*, 378.